ORIGINAL RESEARCH

Engineered hepatitis B virus surface antigen L protein particles for in vivo active targeting of splenic dendritic cells

Hidenori Matsuo[1]
Nobuo Yoshimoto[1]
Masumi Iijima[1]
Tomoaki Niimi[1]
Joohee Jung[2,3]
Seong-Yun Jeong[3]
Eun Kyung Choi[3,4]
Tomomitsu Sewaki[5]
Takeshi Arakawa[6,7]
Shun'ichi Kuroda[1]

[1]Graduate School of Bioagricultural Sciences, Nagoya University, Nagoya, Japan; [2]College of Pharmacy, Duksung Women's University, Seoul, South Korea; [3]Institute for Innovative Cancer Research, ASAN Medical Center, Seoul, South Korea; [4]Department of Radiation Oncology, University of Ulsan College of Medicine, Seoul, South Korea; [5]GenoLac BL Corporation, Okinawa, Japan; [6]COMB, Tropical Biosphere Research Center, [7]Graduate School of Medicine, University of the Ryukyus, Okinawa, Japan

Correspondence: Shun'ichi Kuroda
Department of Bioengineering Sciences, Graduate School of Bioagricultural Sciences, Nagoya University Furo-cho, Chikusa, Nagoya 464-8601, Japan
Tel +81 52 789 5227
Email skuroda@agr.nagoya-u.ac.jp

Abstract: Dendritic cells (DCs) are key regulators of adaptive T-cell responses. By capturing exogenous antigens and presenting antigen-derived peptides via major histocompatibility complex molecules to naïve T cells, DCs induce antigen-specific immune responses in vivo. In order to induce effective host immune responses, active delivery of exogenous antigens to DCs is considered important for future vaccine development. We recently generated bionanocapsules (BNCs) consisting of hepatitis B virus surface antigens that mediate stringent in vivo cell targeting and efficient endosomal escape, and after the fusion with liposomes (LP) containing therapeutic materials, the BNC-LP complexes deliver them to human liver-derived tissues in vivo. BNCs were further modified to present the immunoglobulin G (IgG) Fc-interacting domain (Z domain) derived from *Staphylococcus aureus* protein A in tandem. When mixed with IgGs, modified BNCs (ZZ-BNCs) displayed the IgG Fv regions outwardly for efficient binding to antigens in an oriented-immobilization manner. Due to the affinity of the displayed IgGs, the IgG-ZZ-BNC complexes accumulated in specific cells and tissues in vitro and in vivo. After mixing ZZ-BNCs with antibodies against DCs, we used immunocytochemistry to examine which antibodies delivered ZZ-BNCs to mouse splenic DCs following intravenous injection of the ZZ-BNCs. ZZ-BNCs displaying anti-CD11c monoclonal antibodies (α-CD11c-ZZ-BNCs) were found to accumulate with approximately 62% of splenic DCs, and reside within some of them. After the fusion with liposomes containing antigens, the α-CD11c-ZZ-BNCs could elicit the respective antibodies more efficiently than other nontargeting control vaccines, suggesting that this DC-specific nanocarrier is promising for future vaccines.

Keywords: drug-delivery system, gene-delivery system, liposomes, protein A, vaccine, ZZ domain

Introduction

Dendritic cells (DCs) are a type of antigen (Ag)-presenting cell (APC) that are distributed in lymph nodes, spleen, thymus, skin, and blood.[1,2] APCs incorporate exogenous Ags by endocytosis, execute their processing into fragments, and then immediately display them for recognition by adaptive naïve T cells.[2,3] Subsequently, the T cells activate humoral and cellular immune responses against the exogenous Ags. In particular, DCs are significantly more effective in T cell stimulation than other APCs such as macrophages and B cells,[4,5] indicating that DCs play a central role in immune defense against exogenous pathogens.

Recently, DC-targeting nanocarriers have been developed for effective vaccines using the DC-specific delivery of Ag-encoding genes or exogenous antigens. For example, the replication-defective forms of the lymphocytic choriomeningitis virus,[6,7]

coronavirus,[8] and lentivirus displaying the Sindbis virus glycoprotein[9] have been used for DC-specific gene delivery. However, these vectors present the potential problems commonly observed in viral vectors, including unexpected immunological responses in patients, accidental disturbance of the patients' chromosomes, and unacceptability for Ags other than DNA. Nonviral vectors have also been utilized for delivering Ags to DCs. Nanoparticles consisting of poly(γ-glutamic acid) could target DCs passively through systemic administration.[10] Micelles consisting of poly(ethylene glycol)-based amphipathic polymer accumulated in nearly 20% of DCs in draining lymph nodes following intradermal injection.[11] Liposomes (LPs) and Ags, modified with Fv forms of α-CD11c,[12,13] bacterial flagellin-related peptide,[14] and mannose,[15] could target DCs more efficiently than passive targeting due to their specific interactions with DC surface molecules. Although these nonviral vectors may in part solve the viral vector-related problems described above, they potentially lack the mechanisms for infection and endosomal escape (eg, membrane fusiogenic domain of viral envelope proteins), leading to reduced immunogenicity of Ags due to low recognition efficiency of DCs. Therefore, it is necessary to endow nonviral vectors with both targeting ability and membrane fusiogenic activity in order to develop effective DC-targeting nanocarriers for future vaccines.

Bionanocapsules (BNCs) are approximately 50-nm hollow nanoparticles consisting of about 110 molecules of hepatitis B virus (HBV) surface antigen (HBsAg) L protein and unilamellar LP.[16] BNCs are produced efficiently in recombinant yeast engineered to express the L protein.[17,18] BNCs specifically attach to human hepatic cells via the N-terminal half of the L protein (pre-S1 region), and enter into the cells at the same rate as HBV.[19] Following encapsulation of various materials (eg, genes, proteins, chemical compounds) by electroporation and liposomal fusion, BNCs deliver them specifically to human hepatic cells not only in vitro but also in vivo.[20,21] We have replaced the central part of the pre-S1 region (amino acid residues 51 to 159) of BNC with a tandem form of the IgG Fc-interacting region (Z domain) derived from *Staphylococcus aureus* protein A[22] to generate the ZZ-L protein[23] (Figure 1A). The mutated BNC (ZZ-BNC) can tether IgG Fc regions and display IgG Fv regions outwardly for the effective binding of Ags in an oriented-immobilization manner (Figure 1B),[24] while retaining membrane fusiogenic activity. ZZ-BNCs displaying α-epidermal growth factor receptor (EGFR) antibodies efficiently targeted EGFR-overexpressing glioblastoma in vivo following intracerebroventricular injection.[25] These properties of ZZ-BNCs
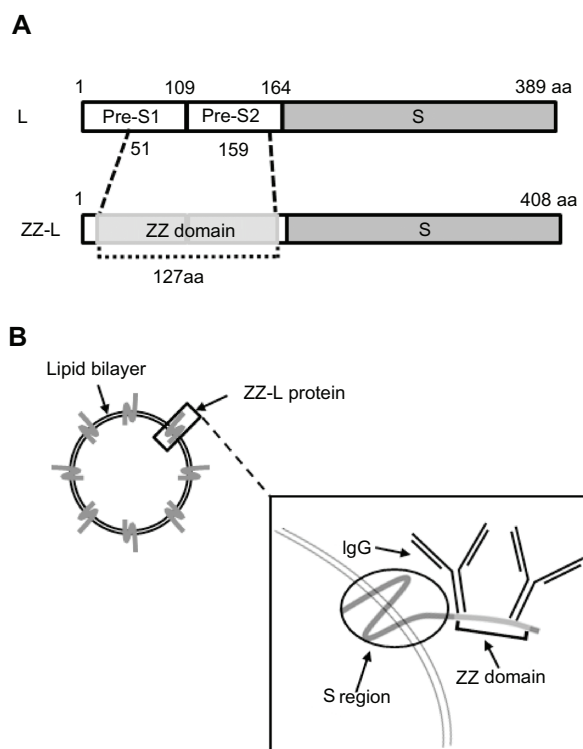
Figure 1 Schematic representation of ZZ-BNCs. (**A**) Molecular organizations of HBsAg L protein (upper) and ZZ-L protein (lower). The numbers indicate amino acid residues (aa) at domain borders. (**B**) Structure of approximately 50-nm diameter ZZ-BNCs. Approximately 120 molecules of ZZ-L protein are embedded in a liposome by integration of their S regions into the lipid bilayer. Two IgGs potentially associate with the ZZ domain, which is displayed on the surface of ZZ-BNCs.
Abbreviations: HBsAg, hepatitis B virus surface antigens; ZZ-BNC, BNC displaying ZZ domains; IgG, immunoglobulin G.

may be useful for active targeting and the introduction of Ags to DCs, making DC-mediated vaccination a promising approach. In this study, ZZ-BNCs displaying α-DC antibodies (α-DC-ZZ-BNCs) were evaluated for both targeting and introduction into splenic DCs in vitro and in vivo. The α-DC-ZZ-BNCs could be used for DC-specific nanocarriers following the fusion with LPs containing antigens.

Material and methods
Materials

BNCs and ZZ-BNCs were overexpressed in *Saccharomyces cerevisiae* AH22R⁻ cells carrying the BNC- and ZZ-BNC-expression plasmids, pGLDLIIP39-RcT[17] and pGLD-ZZ50,[23] respectively. BNCs and ZZ-BNCs were purified as described previously.[18,26] Protein concentrations were determined with a bicinchoninic acid (BCA) protein assay kit (Pierce, Rockford, IL) using bovine serum albumin (BSA; Wako Pure Chemical Industries, Osaka, Japan) as a control protein. BNC was labeled with a Fluorolink Cy5 monofunctional reactive dye (GE Healthcare, Milwaukee, WI) and CF750 NHS ester

(Biotium, Heyward, CA) according to the manufacturer's protocol. Z-averages and ζ-potentials of ZZ-BNCs were measured in water at 25°C with a dynamic light-scattering (DLS) model Zetasizer Nano ZS (Malvern Instruments, Malvern, UK).

Antibodies

Armenian hamster monoclonal α-CD11c IgG (clone N418), rat α-major histocompatibility complex (MHC) class II IgG2b (clone NIMR-4), and Armenian hamster IgG isotype control were purchased from eBioscience (San Diego, CA). Rat α-CD11c IgG2a (clone 223H7) was from Medical and Biological Laboratories (Nagoya, Japan). Rat α-CD86 IgG2b (clone 2D10) was from Southern Biotechnology Associates, Inc (Birmingham, AL). Rat α-CD16/CD32 IgG2b (clone 2.4G2) and isotype controls of rat IgG2a and rat IgG2b were from BD Bioscience Pharmingen (San Diego, CA). Fluorescein isothiocyanate (FITC)-labeled α-CD11c (α-CD11c-FITC, clone N418) was from Miltenyi Biotech (Bergisch Gladbach, Germany).

Quartz crystal microbalance (QCM)

The number of IgG molecules bound to ZZ-BNCs was determined by a quartz crystal microbalance (QCM) model Twin-Q (As One Corp, Osaka, Japan), as described previously.[24] Briefly, the sensor chip of the QCM consisted of a 9-mm-diameter disk made from an AT-cut 27-MHz quartz crystal with gold electrodes on both sides (diameter, 2.5 mm; area, 4.9 mm^2). A frequency change (ΔF) of 1 Hz corresponded to a weight change of 0.6 ng/cm^2. The temperature of the measuring bath (~600 μL) was kept at 25°C. The bath was mixed at 600 rpm with a stirring tube. Measurements were taken in triplicate until a stable frequency (less than ±3 Hz) was observed for >1 minute. Protein samples were dissolved in 500 μL of phosphate-buffered saline (PBS). The sensor chip was treated with ZZ-BNC (4 μg/mL as protein), blocked with Block Ace (2 mg/mL, DS Pharma Biomedical, Osaka, Japan), and then reacted with each IgG isotype control (40 μg/mL).

Preparation of α-DC-ZZ-BNC complexes

Displaying of α-DC IgGs on the surface of ZZ-BNCs was carried out by chemical crosslinking, as described previously.[27] Briefly, 1 μg of each IgG was crosslinked with Cy5- or CF750-labeled ZZ-BNCs (5 μg as protein) in the presence of 50 μM *bis*-sulfosuccinimidyl suberate[3] (BS; Pierce). After incubation at room temperature for 1 hour, 100 μM glycine (pH = 7.5) was added to quench the crosslinking reaction.

Ex vivo attachment assay to splenic DCs

Splenic DCs were isolated from BALB/c female mice (six to eight weeks; Japan SLC, Shizuoka, Japan). Briefly, spleens were treated with a gentleMACS™ dissociator (Miltenyi Biotech) in the presence of 2 mg/mL collagenase D (Roche, Mannheim, Germany). CD11c$^+$ cells were purified from the splenocytes by magnetic cell sorting with MACS® (Miltenyi Biotech) using FcR Blocking Reagent and α-CD11c (clone N418)-labeled magnetic beads. The cell population containing >80% CD11c$^+$ cells was used as splenic DCs for further experiments. DCs (2.5–5.0 × 10^5 cells) were mixed with each Cy5-labeled α-DC-ZZ-BNC complex (1 μg as ZZ-L protein), incubated at 4°C for 30 minutes, and then analyzed with the flow cytometer BD FACScan Canto II (BD Biosciences, San Jose, CA) with linear amplification for forward/side scatter and logarithmic amplification for FITC and Cy5 fluorescence. The FITC-derived fluorescence (emission 520 nm) was excited by a 488-nm laser and Cy5-derived fluorescence (emission 670 nm) was excited by a 633-nm laser.

In vivo imaging analysis

Each mouse was injected intravenously with 100 μL of PBS containing 10 μg (as protein) of CF750-labeled ZZ-BNCs conjugated with each α-DC IgG. After 40 minutes, the mice were sacrificed, and the fluorescent signals for heart, lung, kidney, liver, and spleen were measured using an in vivo imaging system OV-100 (Olympus, Tokyo, Japan). The CF750-derived fluorescence (emission 777 nm) was excited with a xenon lamp and emission filter (from 708 to 752 nm), and obtained through a 770-nm interference barrier filter. To semiquantify the accumulation of CF750-labeled α-DC-ZZ-BNC complexes in each organ, fluorescent signals were measured using WASABI software (Hamamatsu Photonics, Shizuoka, Japan).

In vivo attachment assay to splenic DCs

Cy5-labeled α-DC-ZZ-BNC complexes (10 μg as ZZ-L protein) were injected into mice intravenously. After 40 minutes, the mice were sacrificed and splenocytes were dissociated in MACS buffer with a gentleMACS™ dissociator. An aliquot (190 μL) of cell suspension (2.0–5.0 × 10^6 cells) was mixed with 10 μL of α-CD11c-FITC, incubated at 4°C for 30 minutes, and washed three times with MACS buffer. To evaluate the DC-targeting of each BNC, the cells were subjected to quantitative analysis using the flow cytometer BD FACScan Canto II with linear amplification for forward/side scatter and logarithmic amplification for FITC and Cy5 fluorescence.

The subcellular localization of Cy5-labeled α-DC-ZZ-BNCs complexes was analyzed under a confocal laser scanning microscope (LSM) model FV-1000D (Olympus). Whole cell Z-stacks (each slice = 0.25 μm, total 15 sections) were acquired by the LSM, which was equipped with a 100 × oil objective lens (Olympus).

Preparation of ZZ-BNC-LP complexes

ZZ-BNCs (100 μg as ZZ-L protein) were mixed with 600 μg of cationic LPs (cholesterol: dioleyl phosphatidylethanolamine; [DOPE]: O,O′-ditetradecanoyl-N-(α-trimethylammonioacetyl) diethanolamine chloride [DC-6–14][28] = 3:3:4 [mol:mol:mol]) in Britton–Robinson buffer (pH = 4), and incubated at 37°C for 30 minutes. The complexes of ZZ-BNCs with LPs (ZZ-BNC-LP complexes) were separated by CsCl isopycnic ultracentrifugation (5%–40% (w/v)) in a P40ST rotor at 24,000 rpm at 25°C for 16 hours. The ZZ-BNCs and LPs in each fraction (500 μL) were quantified with a BCA protein assay kit and a cholesterol E-test Wako kit (Wako Pure Chemical Industries), respectively. Fractions containing ZZ-BNC-LP complexes were combined and dialyzed against PBS at 4°C overnight.

Immunization of mice with α-CD11c-ZZ-BNC-LP complexes containing JEV envelope-derived D3 antigen

Japanese encephalitis virus (JEV) envelope-derived D3 antigen was expressed in *Escherichia coli* and purified, as described previously.[29] The D3 antigen (60 μg) was mixed with ZZ-BNC-LP complexes (120 μg of ZZ-L protein, 404 μg of LPs), incubated at room temperature for 1 hour, and then 24 μg of α-CD11c antibodies (clone N418) was conjugated onto the surface of ZZ-BNC-LP-D3 complexes (see Section of Preparation of α-DC-ZZ-BNC complexes). An aliquot of α-CD11c-ZZ-BNC-LP-D3 complexes (20 μg as D3 antigen) was administered to each mouse (BALB/c female, 7 weeks, Japan SLC) intravenously. After 4 weeks, booster immunization was carried out with α-CD11c-ZZ-BNC-LP-D3 complexes (20 μg as D3 antigen). Blood samples were collected from the tail vein for determination of serum α-D3 IgGs at 4 and 6 weeks after the first immunization.

Enzyme-linked immunosorbent assay (ELISA) for serum α-D3 IgGs

The titers of serum α-D3 IgGs were measured by indirect ELISA, as described previously.[29] Briefly, 96-well microtiter plates (Nalge Nunc International, Rochester, NY) were coated with 1 μg/well of the *E. coli*-expressed recombinant D3 protein, and blocked with 10% (w/v) skimmed milk in bicarbonate buffer. Serially diluted antisera and horseradish peroxidase (HRP)-conjugated rabbit anti-mouse IgG (1:4000; Sigma-Aldrich, St Louis, MO) were added to wells, followed by HRP substrate. After 20 minutes of incubation at room temperature, the reaction was stopped by adding 1 N sulfuric acid, and the absorbance was measured at 450 nm (OD450) using a microplate reader (Bio-Rad Laboratories, Redmond, WA).

Results and discussion
Preparation of α-DC-ZZ-BNCs

For efficient DC-targeting of ZZ-BNCs, we examined which commercial α-DC antibodies (ie, α-CD11c [two clones], α-MHC class II, α-CD86, α-CD16/CD32, α-DC-SIGN [two clones], α-CD207 [langerin, two clones]) could detect splenic DCs (CD11c+ population of mouse splenocytes) by flow cytometry. Five of these antibodies (Armenian hamster monoclonal α-CD11c IgG [clone N418], rat α-CD11c IgG2a [clone 223H7], rat α-MHC class II IgG2b [clone NIMR-4], rat α-CD86 IgG2b [clone 2D10], and rat α-CD16/CD32 IgG2b [clone 2.4G2]) were found to label splenic DCs more efficiently than the others. When the amounts of IgGs bound to ZZ-BNCs were determined by QCM,[24] Armenian hamster IgGs were observed to be bound to ZZ-BNCs with high affinity (0.38 ± 0.07 mol per 1 mol ZZ-L protein), and rat IgG2a and IgG2b were weakly bound to ZZ-BNCs (0.02 ± 0.01 and 0.04 ± 0.02 mol per 1 mol ZZ-L protein, respectively). For the generation of stable α-DC-ZZ-BNC complexes, the chemical crosslinker BS3 was added to the mixture of ZZ-BNCs and α-DC antibodies, as described previously.[27] As shown in Table 1, the Z-averages and ζ-potentials of each α-DC-ZZ-BNC complex were less than 100 nm and

Table 1 Z-averages and ζ-potentials of α-DC-ZZ-BNC complexes

BNCs	Antibodies	Z-averages (nm)	ζ-potentials (mV)
ZZ-BNC	None	51.1 ± 0.2	−13.1 ± 3.1
	α-CD11c (clone N418)	66.4 ± 3.8	−20.3 ± 1.5
	α-CD11c (clone 223H7)	52.2 ± 0.1	−18.9 ± 4.5
	α-MHC class II	54.3 ± 1.1	−17.5 ± 2.3
	α-CD86	54.4 ± 1.5	−14.9 ± 1.7
	α-CD16/CD32	51.7 ± 0.4	−14.9 ± 1.0
	Mouse total IgG	152 ± 8.3	−25.2 ± 0.8
BNC	–	69.0 ± 0.2	−14.9 ± 1.3

Notes: Measurements were performed in triplicate. Values are indicated as mean ± SD.
Abbreviations: BNC, bionanocapsule; ZZ-BNC, BNC displaying ZZ domains; IgG, immunoglobulin G; DC, dendritic cell; SD, standard deviation.

negatively charged, respectively, suggesting that each α-DC-ZZ-BNC complex is suitable for in vivo targeting following systemic administration.[30]

Ex vivo attachment of α-DC-ZZ-BNCs to splenic DCs

Recently, our group demonstrated that fluorophore-labeled ZZ-BNC complexes are versatile bioimaging probes for immunocytochemical analyses that can display IgG Fv regions outwardly for the effective binding of Ags.[24,27] Cy5-labeled ZZ-BNCs were mixed with each of five α-DC antibodies, crosslinked with BS[3], and added to the suspension of splenic DCs. Flow cytometric analyses showed that ZZ-BNCs displaying α-CD11c antibodies (clone N418) and α-MHC class II antibodies accumulated on 86% and 84% of splenic DCs, respectively (Figure 2A). Other α-DC antibodies unexpectedly showed lower extents of accumulation, which were similar to those of mouse IgGs and ZZ-BNC alone, but higher than that of BNC alone. These results were

confirmed from the mean fluorescent intensities of DCs incubated with each Cy5-labeled α-DC-ZZ-BNC complex (Figure 2B). The difference in DC accumulation among the α-DC antibodies may be caused by either the number of antibodies on ZZ-BNC or the affinity of each antibody to DCs. Because cell surface molecules on splenic DCs show high affinity to IgGs and ZZ domains,[31–33] ZZ-BNCs displaying mouse IgGs and ZZ-BNC alone may accumulate on DCs. Furthermore, since BNCs and ZZ-BNCs possess high-mannose sugar chains,[17] the mannose receptors of DCs may contribute to the interaction with them.[34]

In vivo distribution of α-DC-ZZ-BNCs

ZZ-BNCs displaying α-CD11c (clone N418) or α-MHC class II antibodies were labeled with CF750 and injected into the tail vein of mice (approximately 10 μg, as ZZ-L protein, per mouse). Because CF750-labeled α-DC-ZZ-BNC complexes were excreted into the bladder within 10 minutes of injection, it was judged that the complexes
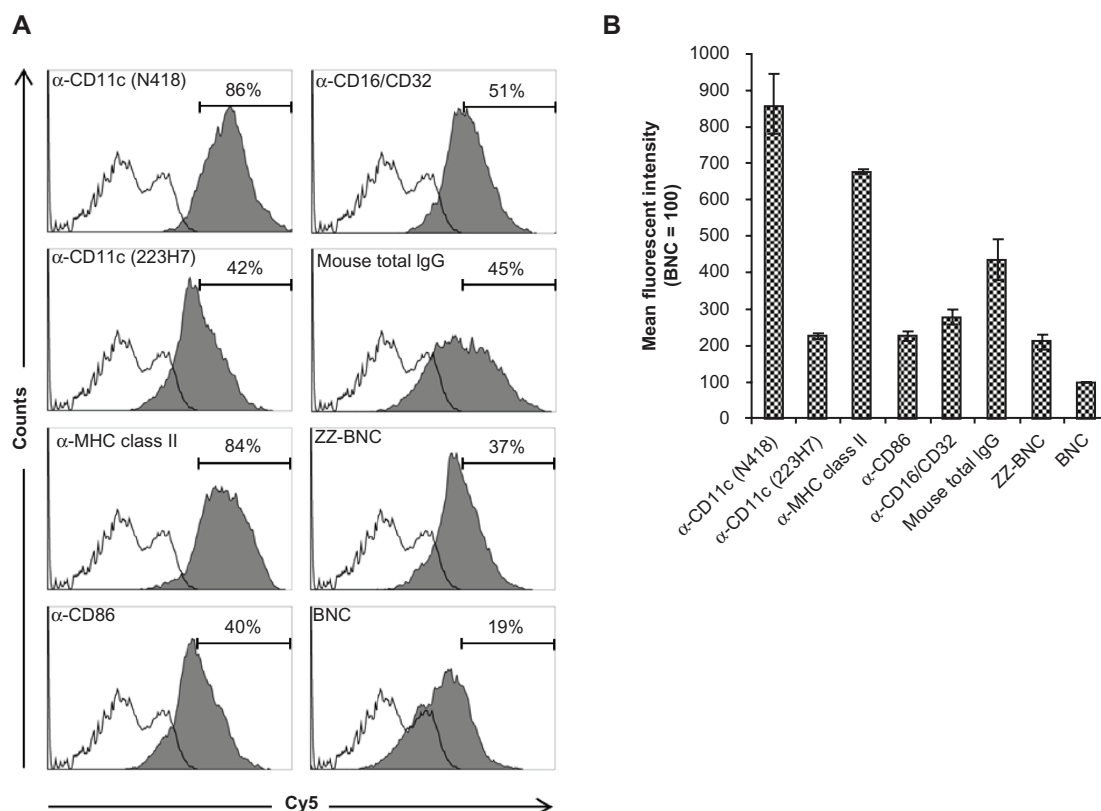

Figure 2 Flow cytometric analysis of ex vivo attachment of α-DC-ZZ-BNCs complexes to splenic DCs. (**A**) Accumulation of Cy5-labeled α-DC-ZZ-BNC complexes to isolated splenic DCs. Splenic DCs were incubated with each Cy5-labeled α-DC-ZZ-BNC complex and subjected to flow cytometric analysis. Fractions of DCs were pre-defined by the forward scatter/side scatter dot plots derived from CD11c+ cells. Distributions of Cy5-derived fluorescence in ZZ-BNC-incubated DCs and untreated DCs are indicated as closed and open histograms, respectively. Antibodies against DCs are shown in the upper left of each panel. The percentages (%) of ZZ-BNC+ cells in DCs are indicated as numbers. (**B**) Mean fluorescent intensities of the Cy5-labeled α-DC-ZZ-BNC complexes in DCs.
Notes: Mean fluorescent intensity derived from DCs incubated with Cy5-labeled BNCs was defined as 100. Measurements were performed in triplicate. Error bars represent the SD.
Abbreviations: DC, dendritic cell; ZZ-BNC, BNC displaying ZZ domains; DC, dendritic cell; SD, standard deviation.

had circulated throughout the whole body by 40 minutes after injection. Mice were sacrificed at 40 minutes after injection and subjected to the extirpation of the heart, lung, kidney, liver, and spleen. Each organ was observed for CF750-derived fluorescence on an OV-100 in vivo imaging system. As shown in Figure 3A, both ZZ-BNCs and BNCs were found to localize in the liver and spleen preferentially. Because the spleen contains a larger number of lymphoid-resident DCs than the liver, and because splenic DCs can induce higher immune responses against exogenous Ags than hepatic DCs,[35] we selected splenic DCs as the target of α-DC-ZZ-BNC for further study. Among the CF750-labeled α-DC-ZZ-BNC complexes, α-CD11c (clone N418) antibodies delivered CF750-labeled ZZ-BNCs to the spleen with the highest specificity (Figure 3B and C). Mouse total IgGs, α-MHC class II antibodies, and ZZ domains could also deliver CF750-labeled ZZ-BNCs to the spleen to some extent, suggesting that these molecules have an affinity to splenic DCs, as described previously.[31–33]

In vivo attachment of α-DC-ZZ-BNCs to splenic DCs

The Cy5-labeled ZZ-BNCs displaying α-CD11c (clone N418) antibodies, α-MHC class II antibodies, and mouse total IgGs were injected into mice intravenously (about 10 μg, as ZZ-L protein, per mouse). At 40 minutes after injection, the mice were sacrificed and their spleens were extirpated. The splenocytes were isolated using a gentleMACS™ dissociator and analyzed by flow cytometry (Figure 4A). The Cy5-labeled α-CD11c (clone N418)-ZZ-BNC complexes were detected in approximately 62% of the CD11c^{+} splenocytes, while the other Cy5-labeled ZZ-BNC complexes, Cy5-labeled ZZ-BNCs, and Cy5-labeled BNCs, were detected in a lower population of CD11c^{+} splenocytes. Moreover, since Cy5-labeled α-CD11c
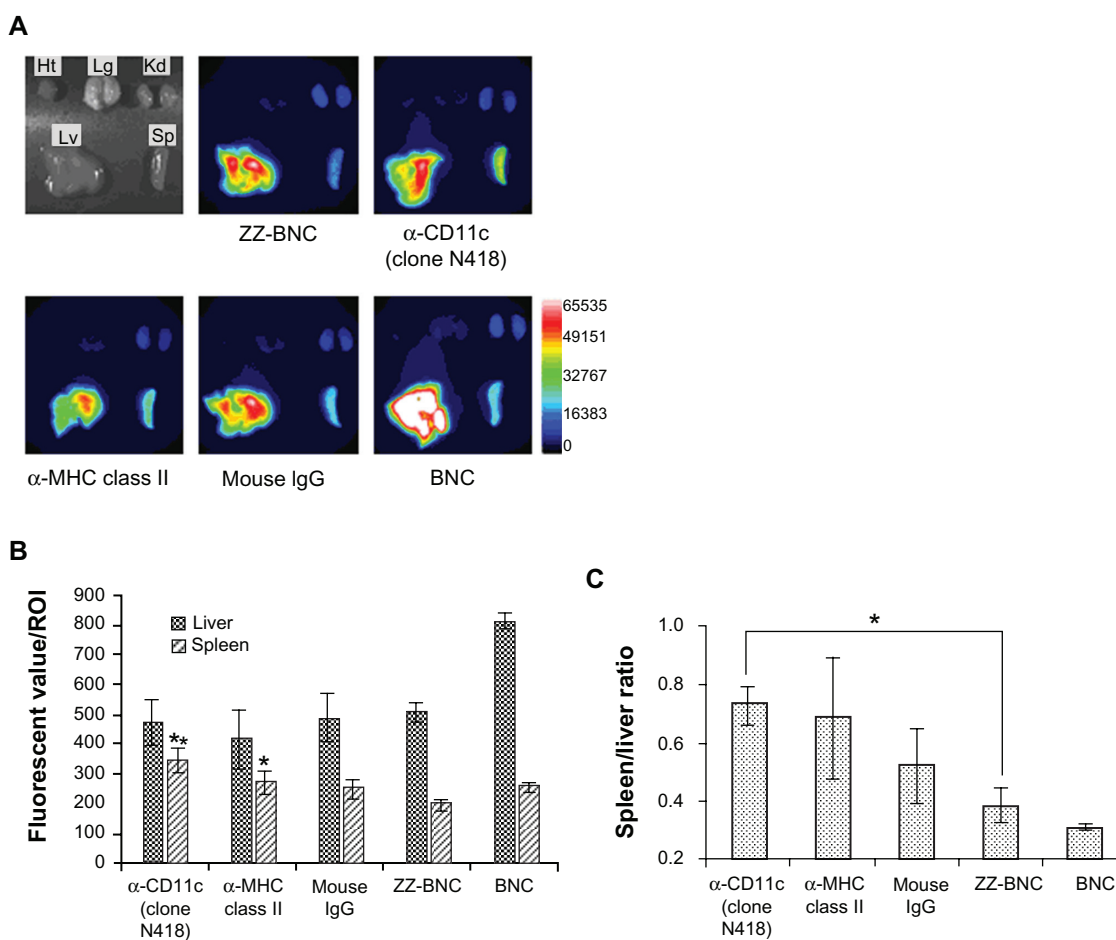

Figure 3 In vivo distribution of CF750-labeled α-DC-ZZ-BNC complexes following intravenous injection into mice. (**A**) CF750-derived fluorescence in each extirpated organ was observed using an OV-100 in vivo imaging system 40 minutes after intravenous injection into mice. (**B**) Fluorescent values of each organ in ROI were analyzed using WASABI software. Measurements were performed in triplicate. Error bars indicate the SD; **$P < 0.01$; *$P < 0.05$. (**C**) Fluorescent ratio between the spleen and liver in ROI was calculated from the average fluorescent values of the spleen and liver. *$P < 0.05$.
Abbreviations: DC, dendritic cell; ZZ-BNC, BNC displaying ZZ domains; Ht, heart; Lg, lung; Kd, kidney; Lv, liver; Sp, spleen; ROI, region of interest; SD, standard deviation.
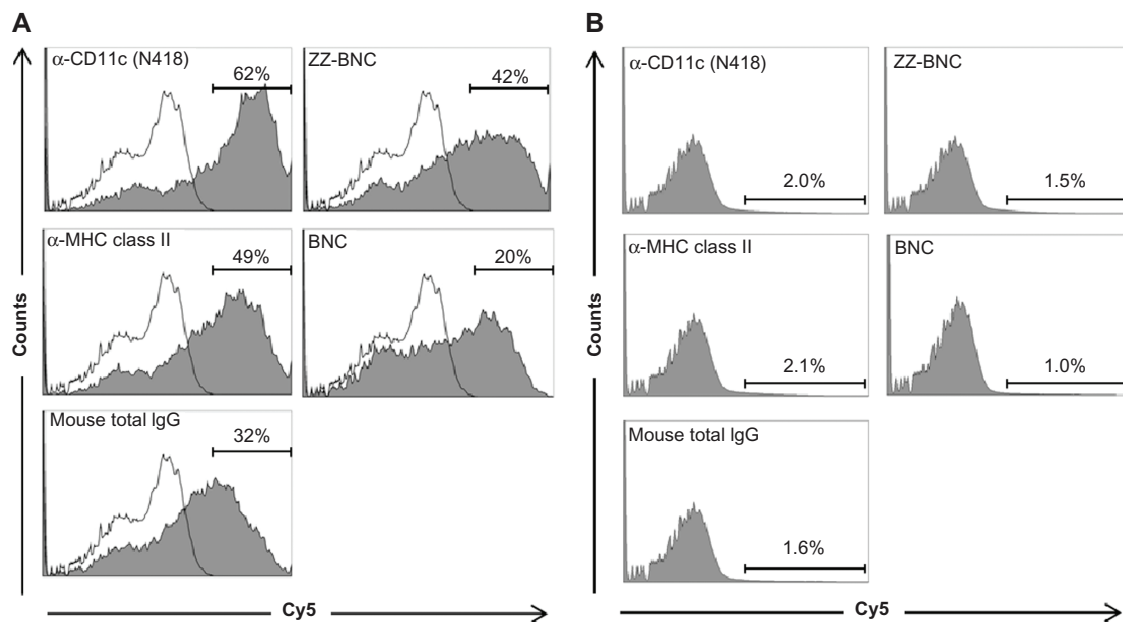
Figure 4 Flow cytometric analysis of in vivo attachment of α-DC-ZZ-BNC complexes to splenic DCs. (**A**) Distributions of Cy5-derived fluorescence in splenic DCs isolated from Cy5-labeled α-DC-ZZ-BNC complex-injected mice and untreated mice are indicated by closed and open histograms, respectively. (**B**) Distributions of Cy5-derived fluorescence in splenic CD11c⁻ cells isolated from Cy5-labeled α-DC-ZZ-BNC complex-injected mice.
Notes: The percentages (%) of ZZ-BNC⁺ cells in DCs and CD11c⁻ cells are indicated as numbers.
Abbreviations: DC, dendritic cell; ZZ-BNC, BNC displaying ZZ domains.

(clone N418)-ZZ-BNC complexes were detected in 2.0% of CD11c⁻ splenocytes (Figure 4B), it was determined that the complexes have high specificity to splenic CD11c⁺ cells in vivo. Next, CD11c⁺ cells were purified from the splenocytes by magnetic cell sorting with MACS using α-CD11c-labeled magnetic beads, stained immunocytochemically with FITC-labeled α-CD11c antibodies, and then observed under LSM (Figure 5). ZZ-BNCs were colocalized with 82.4% ± 10.6% (mean ± SD, N = 73) of CD11c⁺ cells. Z-stack projections of CD11c⁺ cells containing ZZ-BNCs were generated from deconvolved slices

Figure 5 Incorporation of Cy5-labeled α-CD11c (clone N418)-ZZ-BNC complexes by splenic DCs isolated from Cy5-labeled α-DC-ZZ-BNC complex-injected mice.
Notes: Z-stack projections of splenic DCs were generated from deconvolved slices using the maximum intensity criteria. Fluorescence derived from ZZ-BNCs and CD11c molecules is indicated in red and green, respectively. Scale bars, 5 μm.
Abbreviations: DC, dendritic cell; ZZ-BNC, BNC displaying ZZ domains; DIC, differential interference contrast.

using the maximum intensity criteria, indicating that the intravenously injected α-CD11c (clone N418)-ZZ-BNC complexes were immediately incorporated into splenic DCs.

When lymphocytic choriomeningitis viral vectors were injected into mice intravenously, viral particles accumulated in 11% and 60% of splenic DCs on days 3 and 7 after injection.[8] LPs displaying bacterial flagellin-related peptide could accumulate in about 20% of splenic DCs 1 hour after intravenous injection.[14] Moreover, α-CD11c F(ab)²-fused Ags could accumulate in 1.5% and 81.4% of splenic DCs at 4 and 12 hours after subcutaneous injection.[13] These results demonstrated that the α-CD11c-ZZ-BNC complexes could more promptly and efficiently accumulate in splenic DCs (in 62% of CD11c⁺ splenocytes at 40 minutes after intravenous injection) than other DC-targeting nanocarriers. Because ZZ-BNCs could display antibodies in an oriented-immobilization manner and thereby significantly enhance the sensitivity, antigen-binding capacity, and affinity of the antibody itself,[24,26,27] complex formation by α-CD11c antibodies with ZZ-BNCs may improve the molecular recognition between CD11c molecules and DC-targeting nanocarriers.
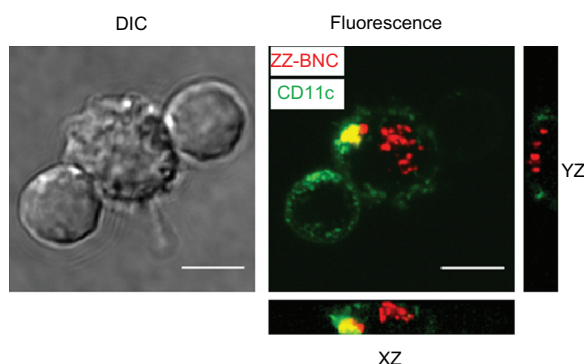
Immunization of mice with α-CD11c-ZZ-BNC-LP-D3 complexes

ZZ-BNCs injected intravenously did not affect the morphology and the cytokine secretions of mouse splenocytes

significantly (data not shown), which led us to examine the efficacy of the α-CD11c-ZZ-BNC complexes for delivering antigens to splenic DC cells in vivo. BNCs were shown to form a stable complex with LP spontaneously and deliver the complex in a cell- and tissue-specific manner in vivo and in vivo.[21] After mixing ZZ-BNCs with cationic LPs, the ZZ-BNC-LP complexes were purified by CsCl isopycnic ultracentrifugation, followed by dialysis against PBS. The complexes consisted of 19.5 μg/mL of ZZ-L protein and 65.6 μg/mL of LPs, of which the Z-average (diameter) and ζ-potential were 426 nm (Polydispersity Index [PDI], 0.331) and −5.76 mV, respectively. For evaluating in vivo delivery specifically to splenic DCs, we chose domain III (D3) of the JEV envelope protein as a control Ag. D3 antigen was expressed in *E. coli* and subsequently purified, as described previously.[29] The ZZ-BNC-LP complex (120 μg as ZZ-L protein, 404 μg as LPs) was allowed to conjugate with 60 μg of D3 antigen by electrostatic interaction and to display 24 μg of α-CD11c antibodies (clone N418) on the complex. The Z-averages and ζ-potentials of α-CD11c-ZZ-BNC-LP-D3 complexes, ZZ-BNC-LP-D3 complexes, and LP-D3 complexes were 455 nm (PDI, 0.398), 324 nm (PDI, 0.261), and 106 nm (PDI, 0.130), and −9.53 mV, −1.87 mV, and 43.4 mV, respectively. While both the diameter and ζ-potential of α-DC-ZZ-BNC complexes were suitable for systemic administration, the conjugation with LPs increased their diameters to greater than 100 nm. However, because the spleen can readily capture nanoparticles of more than 200 nm in diameter from the bloodstream,[36] it was considered that the α-CD11c-ZZ-BNC-LP-D3 complexes could deliver D3 antigens to splenic DCs efficiently following intravenous injection. Mice were immunized intravenously with α-CD11c (clone N418)-ZZ-BNC-LP-D3 complexes (20 μg, as D3 antigen, per mouse) without adjuvant twice with a 4-week interval. D3 alone, LP-D3 complexes, and ZZ-BNC-LP-D3 complexes were used as control vaccines. These control vaccines, containing 20 μg of D3 antigen, were injected into each mouse in the same way. At 4 and 6 weeks after the first immunization, blood samples were collected from the tail vein for determination of serum α-D3 IgGs by ELISA (Figure 6). At 4 weeks, no significant elicitation of α-D3 IgGs was observed in any mouse. Only α-CD11c-ZZ-BNC-LP-D3 complexes elicited high titers of α-D3 IgGs at 6 weeks, while the other control vaccines containing the same amounts of D3 antigen did not. α-CD11c (clone N418)-ZZ-BNCs accumulated in splenic DCs in vivo following intravenous injection (see Figure 5), which strongly suggested that α-CD11c-ZZ-BNC-LP complexes were able to effectively deliver D3 antigens to the inside of splenic DCs.
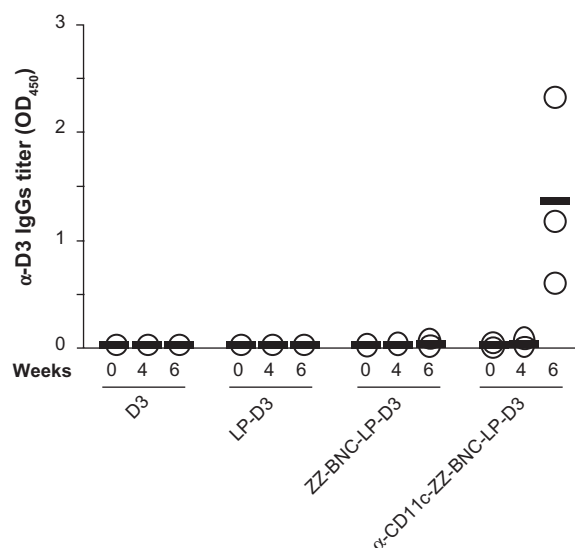

Figure 6 Immunization of mice with α-CD11c-ZZ-BNC-LP-D3 complexes. Titers of α-D3 IgG in sera collected from immunized mice at 0, 4, and 6 weeks were measured by ELISA. Measurements were performed in triplicate. Thick lines indicate average titers from each group.
Abbreviation: ELISA, enzyme-linked immunosorbent assay.

Several lines of evidence have recently indicated that DC targeting mediated by CD11c is superior to that mediated by other molecules. In human monocytes, including DCs, CD11c molecules form heterodimers with CD18 molecules, also known as complement receptor 4 (CR4).[37] Because CR4 mediates phagocytosis, α-CD11c-ZZ-BNC complexes may facilitate the efficient uptake of D3 antigens by DCs, leading to the effective induction of an α-D3 immune response. Moreover, it has been reported that α-CD11c F(ab)2-conjugated Ags accumulated in the splenic marginal zone following intravenous injection and then migrated into the splenic T cell zone, while α-MHC class II F(ab)2-conjugated Ags accumulated in the splenic B cell zone.[38] This result strongly suggested that DCs in the splenic marginal zone were stimulated with Ags in a CD11c-dependent manner and then migrated into the splenic T cell zone. Taken together, the α-CD11c-ZZ-BNC-LP-D3 complexes are postulated to accumulate in splenic DCs, stimulate DCs with D3 antigens, move DCs from the marginal zone to the T cell zone, present fragments of D3 antigen with MHC molecules to T cells along with co-stimulating factors (eg, CD80, CD86), and then induce D3-dependent immune responses including the production of α-D3 IgGs. Regarding the administration route, it is rare to administer vaccines intravenously. We should evaluate whether this vaccine platform could target migratory DCs (eg, Langerhans cells) in mice after intramuscular and subcutaneous administration.

Conclusion

ZZ-BNC is a scaffold for displaying IgGs in an oriented-immobilization manner, thus enhancing the sensitivity, antigen-binding capacity, and affinity of IgG itself. In this study, we evaluated ZZ-BNCs displaying α-CD11c antibodies (clone N418) for in vivo DC-targeting following intravenous injection in mice. The α-CD11c-ZZ-BNC complexes accumulated in about 62% of splenic DCs, and were incorporated by DCs immediately. The α-CD11c-ZZ-BNC complex is a useful probe for in vivo imaging of DCs. Furthermore, the α-CD11c-ZZ-BNC-LP complexes loaded with JEV D3 antigens could elicit α-D3 IgG more efficiently than other nontargeting control vaccines, suggesting that this DC-specific nanocarrier is promising for future vaccines.

Acknowledgments

Disclosure

The authors report no conflicts of interest in this work.

References

1. Trombetta ES, Mellman I. Cell biology of antigen processing in vitro and in vivo. *Annu Rev Immunol*. 2005;23:975–1028.
2. Bancherau J, Briere F, Caux C, et al. Immunobiology of dendritic cells. *Immunology*. 2000;18:767–811.
3. Villadangos JA, Schnorrer P. Intrinsic and cooperative antigen-presenting functions of dendritic-cell subsets in vivo. *Nat Rev Immunol*. 2007;7:543–555.
4. Albert ML, Pearce SF, Francisco LM, et al. Immature dendritic cells phagocytose apoptotic cells via $\alpha_v\beta_5$ and CD36, and cross-present antigens to cytotoxic T lymphocytes. *J Exp Med*. 1998;188:1359–1368.
5. Inaba K, Steinman RM. Accessory cell-T lymphocyte interactions, antigen-dependent and -independent clustering. *J Exp Med*. 1986;163:247–261.
6. Flatz L, Hegazy AN, Bergthaler A, et al. Development of replication-defective lymphocytic choriomeningitis virus vectors for the induction of potent CD8+ T cell immunity. *Nat Med*. 2010;16:339–345.
7. Sevilla N, Kunz S, Holz A, et al. Immunosuppression and resultant viral persistence by specific viral targeting of dendritic cells. *J Exp Med*. 2000;192:1249–1260.
8. Cervantes-Barragan L, Züst R, Maier R. Dendritic cell-specific antigen delivery by coronavirus vaccine vectors induces long-lasting protective antiviral and antitumor immunity. *M Bio*. 2010;1:e00171-10.
9. Yang L, Yang H, Rideout K, et al. Engineered lentivector targeting of dendritic cells for in vivo immunization. *Nat Biotechnol*. 2008;26:326–334.
10. Uto T, Wang X, Sato K, et al. Targeting of antigen to dendritic cells with poly(gamma-glutamic acid) nanoparticles induces antigen-specific humoral and cellular immunity. *J Immunol*. 2007;178:2979–2986.
11. Dane KY, Nembrini C, Tomei AA, et al. Nano-sized drug-loaded micelles deliver payload to lymph node immune cells and prolong allograft survival. *J Control Release*. 2011;156(2):154–160.
12. van Broekhoven CL, Parish CR, Demangel C, Britton WJ, Altin JG. Targeting dendritic cells with antigen-containing liposomes: a highly effective procedure for induction of antitumor immunity and for tumor immunotherapy. *Cancer Res*. 2004;64:4357–4365.
13. Wei H, Wang S, Zhang D, et al. Targeted delivery of tumor antigens to activated dendritic cells via CD11c molecules induces potent antitumor immunity in mice. *Clinical Cancer Res*. 2009;15:4612–4621.
14. Faham A, Altin JG. Antigen-containing liposomes engrafted with flagellin-related peptides are effective vaccines that can induce potent antitumor immunity and immunotherapeutic effect. *J Immunol*. 2010;185:1744–1754.
15. White KL, Rades T, Furneaux RH, Tyler PC, Hook S. Mannosylated liposomes as antigen delivery vehicles for targeting to dendritic cells. *J Pharm Pharmacol*. 2006;58:729–737.
16. Yamada T, Iwabuki H, Kanno T, et al. Physicochemical and immunological characterization of hepatitis B virus envelope particles exclusively consisting of the entire L (pre-S1 + pre-S2 + S) protein. *Vaccine*. 2001;19:3154–3163.
17. Kuroda S, Otaka S, Miyazaki T, Nakao M, Fujisawa Y. Hepatitis B virus envelope L protein particles. Synthesis and assembly in Saccharomyces cerevisiae, purification and characterization. *J Biol Chem*. 1992;267:1953–1961.
18. Jung J, Iijima M, Yoshimoto N, et al. Efficient and rapid purification of drug- and gene-carrying bio-nanocapsules, hepatitis B virus surface antigen L particles, from Saccharomyces cerevisiae. *Protein Expr Purif*. 2011;78:149–155.
19. Yamada M, Oeda A, Jung J, et al. Hepatitis B virus envelope L protein-derived bio-nanocapsules: Mechanisms of cellular attachment and entry into human hepatic cells. *J Control Release*. 2012 10;160(2):322–9.
20. Yamada T, Iwasaki Y, Tada H, et al. Nanoparticles for the delivery of genes and drugs to human hepatocytes. *Nat Biotechnol*. 2003;21:885–890.
21. Jung J, Matsuzaki T, Tatematsu K, Okajima T, Tanizawa K, Kuroda S. Bio-nanocapsule conjugated with liposomes for in vivo pin-point delivery of various materials. *J Control Release*. 2008;126:255–264.
22. Nilsson B, Moks T, Jansson B, et al. A synthetic IgG-binding domain based on staphylococcal protein A. *Protein Eng*. 1987;1:107–113.
23. Kurata N, Shishido T, Muraoka M, et al. Specific protein delivery to target cells by antibody-displaying bionanocapsules. *J Biochem*. 2008;144:701–707.
24. Iijima M, Kadoya H, Hatahira S, et al. Nanocapsules incorporating IgG Fc-binding domain derived from *Staphylococcus aureus* protein A for displaying IgGs on immunosensor chips. *Biomaterials*. 2011;32:1455–1464.
25. Tsutsui Y, Tomizawa K, Nagita M, et al. Development of bionanocapsules targeting brain tumors. *J Control Release*. 2007;122:159–164.
26. Iijima M, Matsuzaki T, Kadoya H, et al. Bionanocapsule-based enzyme-antibody conjugates for enzyme-linked immunosorbent assay. *Anal Biochem*. 2010;396:257–261.
27. Iijima M, Matsuzaki T, Yoshimoto N, Niimi T, Tanizawa K, Kuroda S. Fluorophore-labeled nanocapsules displaying IgG Fc-binding domains for the simultaneous detection of multiple antigens. *Biomaterials*. 2011;32:9011–9020.
28. Kikuchi A, Aoki Y, Sugaya S. Development of novel cationic liposomes for efficient gene transfer into peritoneal disseminated tumor. *Hum Gene Ther*. 1999;10:947–955.
29. Tafuku S, Miyata T, Tadano M, et al. Japanese encephalitis virus structural and nonstructural proteins expressed in *Escherichia coli* induce protective immunity in mice. *Microbes Infect*. 2011;4–11.

30. Moghimi SM, Hunter AC, Murray JC. Long-circulating and target-specific nanoparticles: theory to practice. *Pharmacol Rev*. 2001;53:283–318.

31. de Jong JMH, Schuurhuis D, Ioan-Facsinay A, et al. Murine Fc receptors for IgG are redundant in facilitating presentation of immune complex derived antigen to CD8+ T cells in vivo. *Mol Immunol*. 2006;43:2045–2050.

32. Fournier B, Philpott DJ. Recognition of *Staphylococcus aureus* by the innate immune system. *Clin Microbiol Rev*. 2005;18:521–540.

33. Ding X, Yang W, Shi X, et al. TNF receptor 1 mediates dendritic cell maturation and CD8 T cell response through two distinct mechanisms. *J Immunol*. 2011;187:1184–1191.

34. Burgdorf S, Lukacs-Kornek V, Kurts C. The mannose receptor mediates uptake of soluble but not of cell-associated antigen for cross-presentation. *J Immunol*. 2006;176:6770–6776.

35. Pillarisetty VG, Shah AB, Miller G, Bleier JI, DeMatteo RP. Liver dendritic cells are less immunogenic than spleen dendritic cells because of differences in subtype composition. *J Immunol*. 2004;172: 1009–1017.

36. Klibanov AL, Maruyama K, Beckerleg AM, Torchilin VP, Huang L. Activity of amphipathic poly(ethylene glycol) 5000 to prolong the circulation time of liposomes depends on the liposome size and is unfavorable for immunoliposome binding to target. *Biochim Biophys Acta*. 1991;1062:142–148.

37. Keizer GD, Te Velde AA, Schwarting R, Figdor CG, De Vries JE. Role of p150,95 in adhesion, migration, chemotaxis and phagocytosis of human monocytes. *Eur J Immunol*. 1987;17:1317–1322.

38. Castro FVV, Tutt AL, White AL, et al. CD11c provides an effective immunotarget for the generation of both CD4 and CD8 T cell responses. *Eur J Immunol*. 2008;38:2263–2273.